




Article

A Novel Light-Emitting Diode Streetlight Driver Circuit Applied to a Direct Current-Input Voltage Source

Chun-An Cheng , Chien-Hsuan Chang , Hung-Liang Cheng , En-Chih Chang *, You-Ruei Lin and Long-Fu Lan

Department of Electrical Engineering, I-Shou University, Kaohsiung City 84001, Taiwan; cacheng@isu.edu.tw (C.-A.C.); chchang@isu.edu.tw (C.-H.C.); hlcheng@isu.edu.tw (H.-L.C.); isu10901006m@cloud.isu.edu.tw (Y.-R.L.); isu11001004m@cloud.isu.edu.tw (L.-F.L.)

* Correspondence: enchihchang@isu.edu.tw; Tel.: +886-7-6577711 (ext. 6642)

Abstract: With the global advocacy of green lighting and the urgent need for energy saving and carbon reduction, more and more street lighting applications have entered the era of being replaced by light-emitting diode (LED) lighting sources. This paper presents a new LED streetlight driving circuit applied to a direct current (DC)-input voltage source, which consists of a buck converter combined with a flyback converter to reduce the number of circuit components required and to recover the leakage energy of the transformer to improve energy conversion efficiency. In addition, this study also completed the analysis of the operational principle of the new LED streetlight driving circuit, and developed a prototype LED streetlight driver with DC-input voltage of 48V and output power of 72 W (36 V/2 A). Finally, the measurement results of the prototype circuit show that the output voltage ripple rate was less than 15%, the output current ripple rate was less than 6%, and the circuit efficiency was as high as 91%.

Keywords: converter; direct current (DC)-input voltage source; driver circuit; light-emitting-diode (LED); streetlight



Citation: Cheng, C.-A.; Chang, C.-H.; Cheng, H.-L.; Chang, E.-C.; Lin, Y.-R.; Lan, L.-F. A Novel Light-Emitting Diode Streetlight Driver Circuit Applied to a Direct Current-Input Voltage Source. *Sustainability* **2023**, *15*, 10934. <https://doi.org/10.3390/su151410934>

Academic Editor: Lin Lu

Received: 28 March 2023

Revised: 7 July 2023

Accepted: 10 July 2023

Published: 12 July 2023



Copyright: © 2023 by the authors. Licensee MDPI, Basel, Switzerland. This article is an open access article distributed under the terms and conditions of the Creative Commons Attribution (CC BY) license (<https://creativecommons.org/licenses/by/4.0/>).

1. Introduction

Road safety is a top priority when designing roads, not only for motorists, but also for pedestrians. Street lighting is a key contributor to road safety. Proper street lighting can improve visibility, make navigation easier, keep road users and pedestrians safe, and reduce crime. Street lighting systems facilitate the use of roadways for drivers and pedestrians. In addition to public safety, they also promote the effectiveness of roads as a means of transportation [1,2].

A high-pressure mercury lamp is a type of gas discharge lamp, which is a light source containing mercury vapor inside; it produces bright light in the form of gas discharge. High-pressure mercury lamps have the advantage of high luminous efficiency and long service life. As the lamp of a high-pressure mercury street lamp contains mercury, it has associated environmental pollution problems; high-pressure mercury street lamps also have high energy consumption, light decay, and are not environmentally-friendly lamps. Therefore, their use has been greatly reduced. A high-pressure sodium lamp is also a type of gas discharge lamp, which is not only used as a light source for road lighting, but also for lighting scenes and other occasions. Both high-pressure mercury lamps and high-pressure sodium lamps are high energy-consuming street lighting sources, commonly used for outdoor lighting on roads, plazas, streets, stadiums, ball fields, and parks [3,4].

Streetlights are vital to modern life and are an important infrastructure for social security and road safety. However, streetlights are high energy-consuming facilities for long-term lighting, which are a burden to environmental protection, electricity consumption, and government finance. In line with the global trend of clean energy, and taking into

account energy saving and carbon reduction, as well as reducing the financial burden of the government, streetlights, as an important component of urban lighting, can meet the needs of environmental protection and energy saving using energy-saving and high-efficiency light sources. LED streetlights, compared with traditional high-pressure mercury and high-pressure sodium lamps, have a longer life span, lower energy consumption, high lighting efficiency, and also provide a clearer view of the road at night and reduce maintenance costs. As well, the costs of installing and maintaining LED streetlights have virtually bottomed out. Consequently, LED streetlights have replaced traditional sources of street lighting and play an important role in energy-efficient outdoor lighting [5–10]. Replacing old energy-consuming traditional streetlight sources with energy-efficient LED lights not only reduces the environmental pollution caused by high-pressure mercury lamps and carbon dioxide emissions, but also significantly reduces the power consumption of streetlights and lowers the power generation load and costs for power companies. In addition, complete replacement using energy-saving streetlights can provide a safer and more comfortable living environment and quality of life for citizens, and enable a city to move towards becoming a green city with environmental protection, energy savings, and low-carbon emissions [11–15].

Solar energy is an inexhaustible sustainable source of energy. Solar photovoltaic panels make it possible to convert solar energy into electric energy for streetlights. During the day, energy from sunlight is captured by solar photovoltaic panels and converted into electrical energy stored in the battery, and the energy of the battery can be used to power streetlights at night [16–22]. The literature describes some LED driver circuits that are applied to a DC-input voltage source, such as a solar photovoltaic panel or a battery, suitable for powering LED street lighting applications [23–29]. Reference [27] proposed a Zeta/flyback integrated DC-to-DC converter applied to photovoltaic power generation arrays. The integrated converter combined a Zeta converter with a flyback converter, and the photovoltaic power generation array was used as the input voltage source for LED street lighting systems or digital signage. A battery charger and discharger are required when solar photovoltaic panels are installed in an LED illumination system. In the presented solar photovoltaic panel-powered LED lighting system, a Zeta converter was used as a battery charger and a flyback converter was used as a battery discharger due to its simple circuit topology.

Reference [28] presented a full-bridge resonant DC-to-DC converter as an LED driver circuit. In this circuit, an LED light was powered by two voltage sources connected in series. One of the voltage sources supplied power directly to the main lamp, and the other delivered low power across the full bridge for regulation. The presented driver utilized the fifth harmonic component in the bridge output voltage, which reduced the size of the reactive components and enabled lower switching losses in the full bridge to achieve high efficiency. Reference [29] presented a two-stage DC-to-DC driver circuit for LED lighting applied to automotive headlights. The front stage was a step-up DC-to-DC converter, and the rear stage was a step-down converter. The entire driver circuit consisted of a boost converter and two buck converters, and was used to drive two sets of automotive headlight LED arrays.

A review of driver circuits for LED lighting applications classified according to whether the topology is isolated or non-isolated is presented in [30]. For basic isolated topology applied to a DC-input voltage source for LED streetlight applications, the main circuit is typically a flyback converter with good electrical isolation characteristics. The disadvantage of the flyback converter is its low transformer utilization due to its unidirectional operation; a snubber circuit is recommended to discharge the energy stored in the leakage inductor of the transformer when the power switch is turned off. For non-isolated converters that are applied to DC-input voltage sources and supply power for LED streetlight applications that are lower than the input voltage level, the main circuits are generally buck converters and buck-boost converters. In addition, buck converters have the attractive features of non-inverting output and continuous output current compared to buck-boost converters. Therefore, this study proposed and developed a novel driver circuit applied to a DC-

input voltage source for LED streetlight applications, which combines a buck converter with a flyback converter into a single-stage single-switch non-isolated buck-flyback power converter. In addition, the proposed driver circuit is suitable for applications where the rated voltage of the LED is lower than the DC-input voltage level, and can recover the energy stored in the leakage inductance of the transformer without using a snubber circuit in order to improve the circuit efficiency.

This paper is organized as follows. Section 2 describes and analyzes operational modes of the proposed LED streetlight driver circuit applied to a DC-input voltage source. Section 3 presents design considerations regarding the proposed LED streetlight driver circuit. In Section 4, experimental results for the prototype LED streetlight driver circuit applied to a DC-input voltage source are demonstrated. Finally, conclusions and future work are presented in Section 5.

2. Descriptions and Operational Modes Analysis of the Proposed LED Streetlight Driver Circuit Applied to a DC-Input Voltage Source

Figure 1 shows the proposed driver circuit applied to a DC-input voltage source to supply an LED streetlight module, which integrates a DC–DC buck converter with a DC–DC flyback converter into single-stage power conversion topology and includes a power switch, S_B ; two diodes, D_B and D_F ; a transformer, T_R , with a magnetizing inductor, L_M , and a leakage inductor, L_{lk} ; two output capacitors, C_{O1} and C_{O2} ; and the LED streetlight module. In addition, the magnetizing inductor, L_M , was designed to operate in continuous conduction mode (CCM), and the proposed driver circuit recycles energy stored in the leakage inductor, L_{lk} , of the transformer, T_R , in order to improve circuit efficiency.

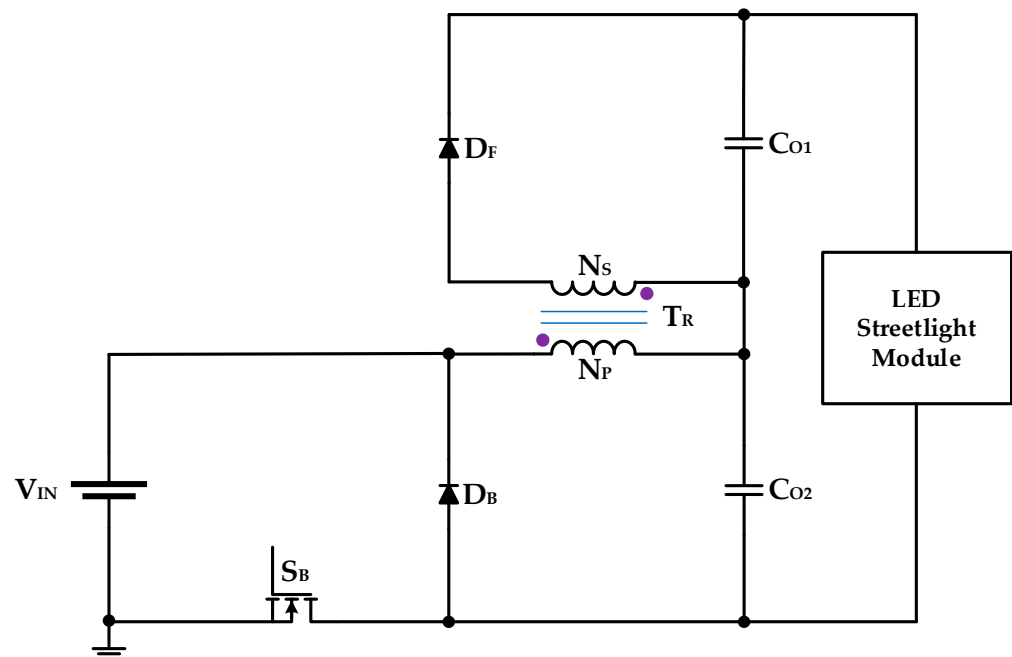


Figure 1. The proposed integrated streetlight driver circuit applied to a DC-input voltage source.

Figure 2 shows the equivalent circuit of the proposed LED streetlight driver applied to a DC-input voltage source, obtained while analyzing the operational modes. In order to analyze the circuit operation of the proposed LED streetlight driver, the following assumptions were made:

- The magnetizing inductor, L_M , of the transformer, T_R , is designed to operate in continuous conduction mode, and L_{lk1} and L_{lk2} are the primary-side leakage inductance and the secondary-side leakage inductance of the transformer, T_R , respectively.
- Assuming that the capacity of energy storage capacitors C_{O1} and C_{O2} is large enough, the output voltage can be regarded as a constant value.

(c) The rest of the circuit elements are considered ideal.

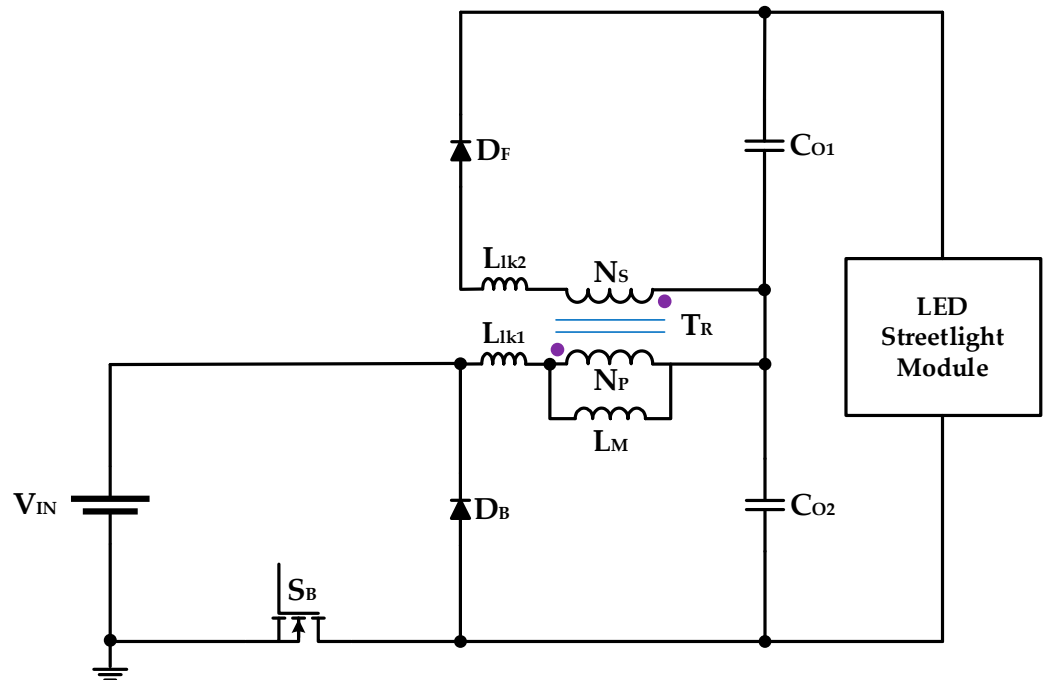


Figure 2. Equivalent circuit of the proposed LED streetlight driver powered by DC voltage.

Figures 3–7 show the operating modes and key waveforms of the LED streetlight driver applied to a DC-input voltage source; the operational analysis is described in detail below.

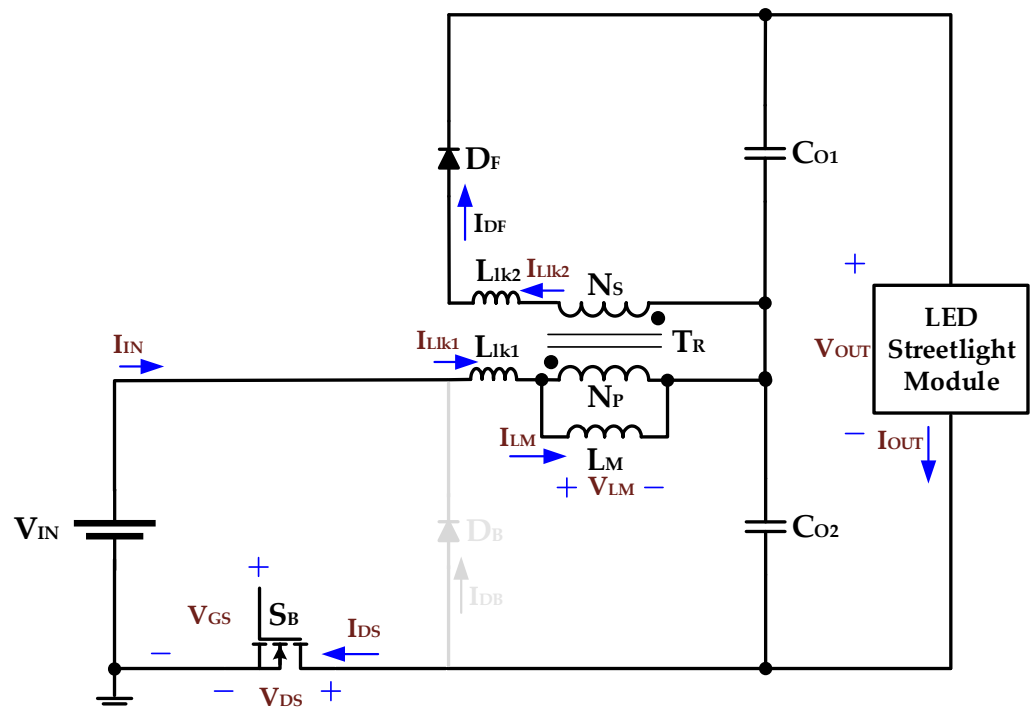


Figure 3. Equivalent circuit of *operational mode 1* in the proposed LED streetlight driver powered by DC voltage.

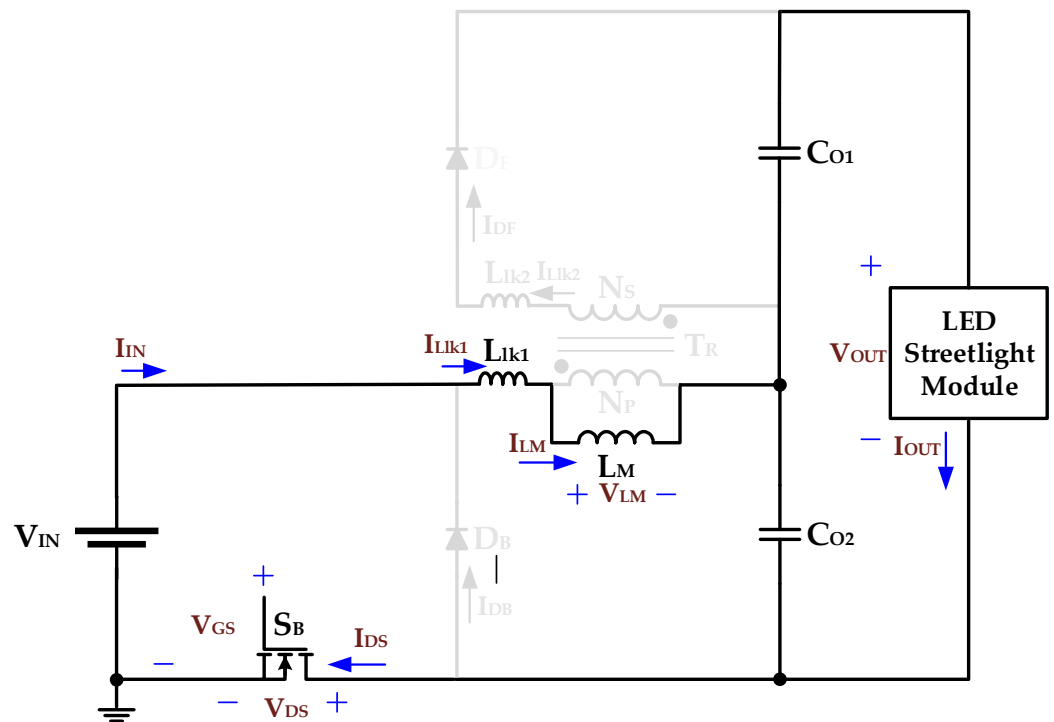


Figure 4. Equivalent circuit of *operational mode 2* in the proposed single-stage LED streetlight driver powered by DC voltage.

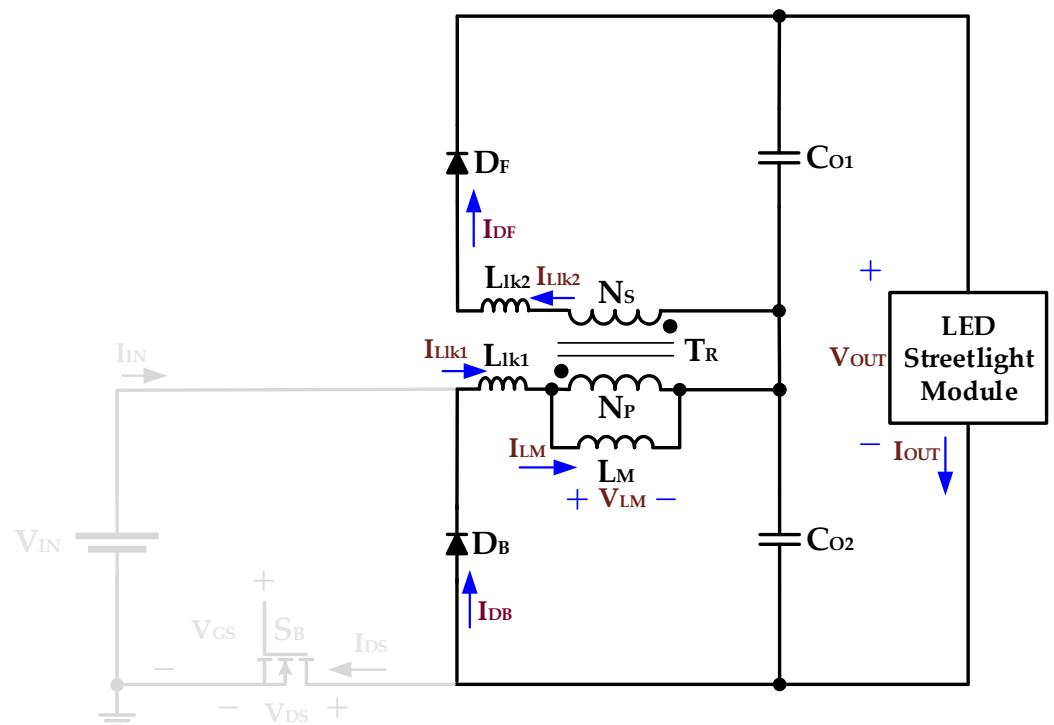


Figure 5. Equivalent circuit of *operational mode 3* in the proposed LED streetlight driver powered by DC voltage.

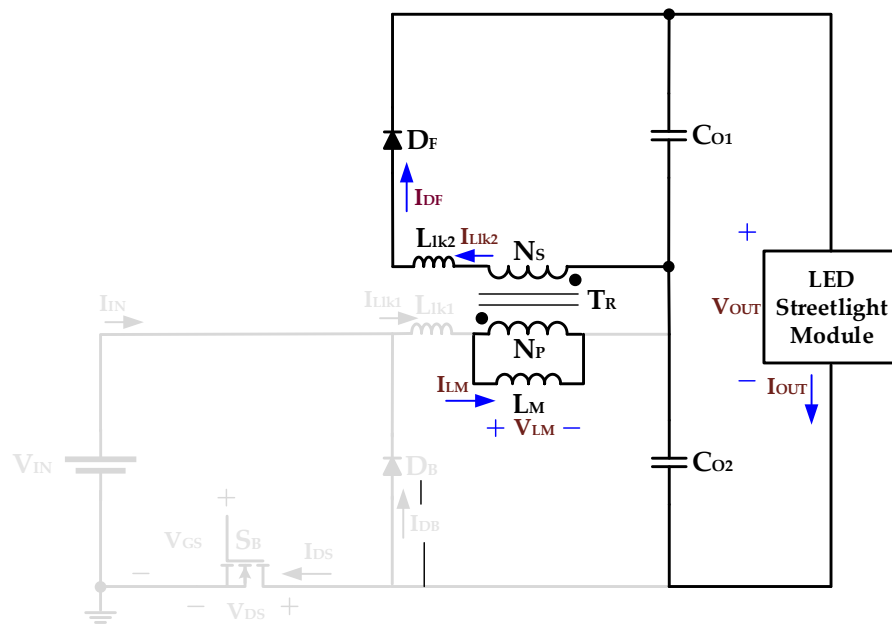


Figure 6. Equivalent circuit of *operational mode 4* in the proposed LED streetlight driver powered by DC voltage.

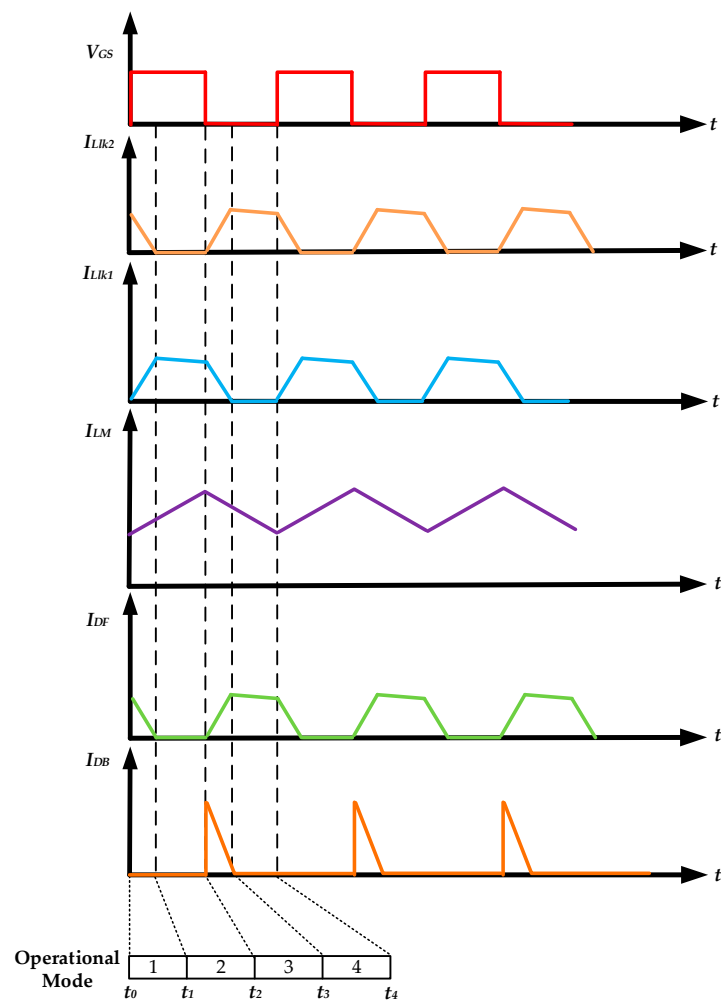


Figure 7. Key waveforms of the proposed LED streetlight driver applied to a DC-input voltage source.

Operation Mode 1 ($t_0 \leq t < t_1$): Figure 3 is an equivalent circuit diagram of *operation mode 1* of the proposed LED streetlight driver circuit powered by DC voltage. At time t_0 , the power switch S_B is turned on, the diode D_B is reverse biased, and the input voltage source V_{IN} provides energy to the magnetizing inductor L_M , the primary-side leakage inductance L_{lk1} , and the energy storage capacitor C_{O1} through the switch S_B . The diode D_F continues the previous mode and presents a forward bias conduction, and the energy is released from the secondary-side leakage inductance L_{lk2} to the LED streetlight module through the diode D_F . When the secondary-side leakage inductance current I_{Llk2} is equal to zero at t_1 , *operation mode 1* ends.

Operational Mode 2 ($t_1 \leq t < t_2$): Figure 4 is an equivalent circuit diagram of *operation mode 2* of the proposed LED streetlight driver circuit powered by DC voltage. At t_1 , the power switch S_B is continuously turned on and the input voltage source V_{IN} continues to provide energy to the magnetizing inductor L_M , the primary-side leakage inductance L_{lk1} , and the capacitor C_{O1} through the power switch S_B . At the same time, the energy storage capacitors C_{O1} and C_{O2} provide energy to the LED streetlight module. When the power switch S_B is turned off at t_2 , *operation mode 2* ends.

Operational Mode 3 ($t_2 \leq t < t_3$): Figure 5 is an equivalent circuit diagram of *operation mode 3* of the proposed LED streetlight driver circuit powered by DC voltage. At t_2 , after the power switch S_B is turned off, the diode D_B is in a state of forward bias, and the magnetizing inductor L_M and the primary-side leakage inductance L_{lk1} provide energy to the energy storage capacitors C_{O1} and C_{O2} , the secondary-side leakage inductance L_{lk2} , and the LED streetlight module through diodes D_B and D_F . When the primary-side leakage inductance current i_{Llk1} is equal to zero at t_3 , *operational mode 3* ends.

Operational Mode 4 ($t_3 \leq t < t_4$): Figure 6 is an equivalent circuit diagram of *operation mode 4* of the proposed LED streetlight driver circuit powered by DC voltage. At t_3 , the power switch S_B is still off, and the magnetizing inductor L_M and the secondary-side leakage inductance L_{lk2} provide energy to the capacitors C_{O1} and C_{O2} , as well as the LED streetlight module, via the diode D_F . Energy storage capacitors C_{O1} and C_{O2} continuously provide energy to the LED streetlight module. When the power switch S_B is turned on again at t_4 , *operation mode 4* ends, and the circuit returns to *operation mode 1*.

3. Design Considerations Regarding Magnetizing Inductor L_M and Output Capacitors C_{O1} and C_{O2} in the Proposed LED Streetlight Driver Circuit

According to the volt-second balance theorem, the voltage occurred on the magnetizing inductor L_M multiplied by the turn-on time of the switch is equal to the voltage occurred on the magnetizing inductor L_M multiplied by the turn-off time of the switch, and can be expressed using the following formula:

$$V_{IN} \times D \times T_S = \frac{N_P}{N_S} \times \frac{V_{OUT}}{2} \times (1 - D) \times T_S \quad (1)$$

where D is the duty cycle of the power switches and T_S is the switching period.

The relationship between the output voltage V_{OUT} and the input voltage V_{IN} can be expressed as

$$\frac{V_{OUT}}{V_{IN}} = \frac{N_S}{N_P} \times \frac{2D}{1 - D} \quad (2)$$

The peak-to-peak value of the magnetizing inductor ΔI_{LM} can be expressed as

$$\Delta I_{LM} = \frac{V_{IN} \times D \times T_S}{L_M} = \frac{V_{OUT} \times N_P \times (1 - D) \times T_S}{2 \times L_M \times N_S} \quad (3)$$

In the boundary case between continuous conduction mode and discontinuous conduction mode, the average value of the magnetizing inductor current I_{LMB} can be expressed as

$$I_{LMB} = I_{OB} = \frac{\Delta I_{LM}}{2} \quad (4)$$

Therefore, in order to operate in continuous conduction mode so that the magnetizing inductor current does not drop to zero, the design consideration of the output current I_O is required to be larger than I_{LMB} , as shown below:

$$I_O > I_{LMB} = I_{OB} = \frac{V_{OUT} \times N_P \times (1-D) \times T_S}{2 \times 2 \times L_{MB} \times N_S} \quad (5)$$

Therefore, the magnetizing inductor L_M is required to be greater than the magnetizing inductor in the boundary conduction mode L_{MB} , and can be expressed as the following formula:

$$\begin{aligned} L_M > L_{MB} &= \frac{V_{OUT} \times N_P \times (1-D) \times T_S}{2 \times 2 \times I_{OB} \times N_S} \\ &= \frac{V_{OUT} \times N_P \times (1-D)}{2 \times 2 \times I_{OB} \times N_S \times f_s} \end{aligned} \quad (6)$$

According to Equation (6), Figure 8 shows the relationship between the magnetizing inductor in the boundary conduction mode L_{MB} and the duty cycle D at different switching frequencies.

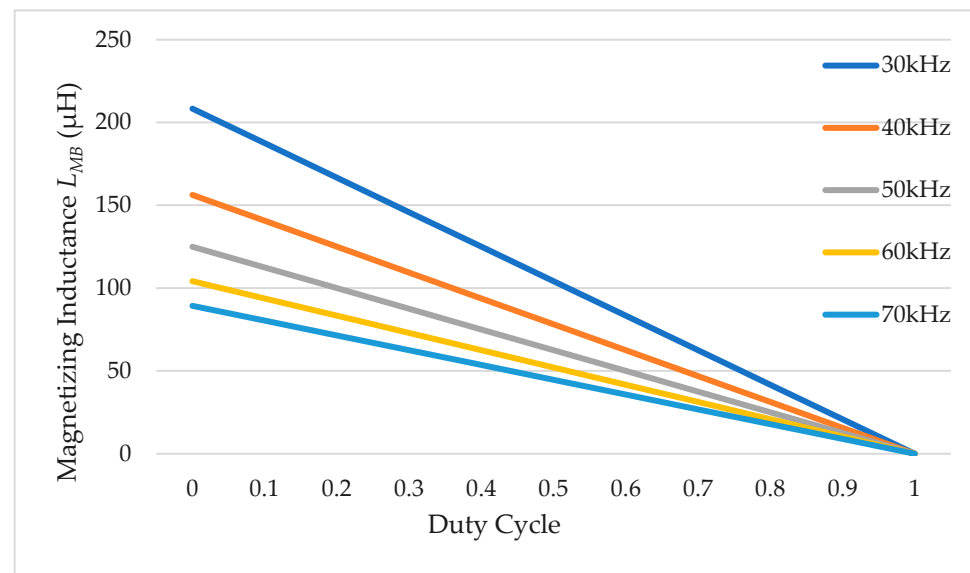


Figure 8. Magnetizing inductor in the boundary conduction mode L_{MB} versus the duty cycle D under different switching frequencies f_s .

Assume that the average output current I_{OB} in the boundary condition is 0.8 times the average output current I_O , and the value of the magnetizing inductor in the boundary conduction mode L_{MB} can be calculated as follows, using Equation (6) with a V_{OUT} of 36 V, an N_P of 10, an N_S of 9, an I_{OB} of 1.6 A, and an f_s of 50 kHz.

$$L_{LMB} = \frac{V_{OUT} \times N_P \times (1-D)}{2 \times 2 \times I_{OB} \times N_S \times f_s} = \frac{36 \times 10 \times (1-0.3)}{2 \times 2 \times 1.6 \times 9 \times 50,000} = 87.5 \mu\text{H}$$

In order to allow the magnetizing inductor current to operate in continuous conduction mode when implementing the circuit, the magnetizing inductor L_M was selected as 100 μH .

Regarding the design of the output capacitors C_{O1} and C_{O2} , the peak-to-peak value of the output voltage ripple ΔV_{OUT} of the output capacitor under continuous conduction mode can be written as

$$\Delta V_{OUT} = \frac{\Delta Q}{C_{O1}} = \frac{2}{C_{O1}} \times \frac{1}{2} \times \frac{\Delta I_{LM}}{2} \times \frac{T_S}{2} = \frac{\Delta I_{LM} \times T_S}{4 \times C_{O1}} \quad (7)$$

Substituting Equation (3) into Equation (7), the expression of the output voltage ripple ΔV_{OUT} can be obtained using

$$\Delta V_{OUT} = \frac{V_{OUT} \times N_P \times (1 - D) \times T_S^2}{16 \times L_M \times C_{O1} \times N_S} \quad (8)$$

The percentage of the output voltage ripple $\Delta V_{OUT}/V_{OUT}$ can be expressed as

$$\frac{\Delta V_{OUT}}{V_{OUT}} = \frac{N_P \times (1 - D) \times T_S^2}{16 \times L_M \times C_{O1} \times N_S} \times 100\% \quad (9)$$

After calculating Equation (9), the design expressions of output capacitors C_{O1} and C_{O2} can be obtained using

$$C_{O1} = C_{O2} = \frac{N_P \times (1 - D) \times V_{OUT}}{16 \times L_M \times N_S \times f_S^2 \times \Delta V_{OUT}} \quad (10)$$

Substituting the circuit parameters into Equation (10), with a V_{OUT} of 36 V, an N_P of 10, an N_S of 9, an f_S of 50 kHz, an L_M of 100 μH , and a ΔV_{OUT} of 0.5 V, the values of capacitors C_{O1} and C_{O2} can be obtained as follows:

$$C_{O1} = C_{O2} = \frac{N_P \times (1 - D) \times V_{OUT}}{16 \times L_M \times N_S \times f_S^2 \times \Delta V_{OUT}} = \frac{10 \times (1 - 0.3) \times 36}{16 \times 100 \times 10^{-6} \times 9 \times 50,000^2 \times 0.5} = 22.85 \mu\text{F}$$

In order to reduce the ripple of the output voltage when implementing the circuit, the output capacitors C_{O1} and C_{O2} were selected as 220 μF .

4. Experimental Results of Prototype LED Streetlight Driver Circuit Applied to a DC-Input Voltage Source

Figure 9 presents a photograph of the LED streetlight module used for the experiment. The specifications of the LED streetlight module used in the experiment are as follows: the rated power was 72 W, the rated input voltage was 36 V, the rated input current was 2 A, the luminous flux was 6000 lm, the luminous efficiency was 63.7 lm/W, the color temperature ranged between 5500 K~6500 K, the weight was 8.6 kg, and the service life of the LED streetlight module was longer than 50,000 h.



Figure 9. Photograph of the LED streetlight module used for the experiment in this study.

A prototype driver circuit from a DC-input voltage of 48 V was successfully implemented and tested for powering a 72 W-rated LED streetlight module with an output rated voltage of 36 V and an output rated current of 2 A. Tables 1 and 2 show the specifications

and key components, respectively, used in the proposed LED streetlight driver circuit applied to a DC-input voltage source.

Table 1. Specifications of the proposed LED streetlight driver circuit applied to a DC-input voltage source.

Parameter	Value
DC-Input Voltage Source V_{IN}	48 V
Rated Output Power P_O	72 W
Rated Output Voltage V_O	36 V
Rated Output Current I_O	2 A

Table 2. Key components used in the proposed LED streetlight driver circuit applied to a DC-input voltage source.

Component	Value
Diodes D_1, D_2	SB1060FCT
Power Switches S_B	STF13NM60N
Transformer T_R	
Magnetized Inductor L_M	100 μ H
Leakage Inductance in the Primary-Side L_{lk1}	1.86 μ H
Leakage Inductance in the Secondary-Side L_{lk2}	1.32 μ H
Turns Ratio $N_P:N_S$	10:9
Output Capacitors C_{O1}, C_{O2}	220 μ F/100 V

Figure 10 presents the measured input voltage V_{IN} and input current I_{IN} ; their measured mean values were 47.61 V and 2.101 A, respectively. The measured switch voltage V_{DS} and switch current I_{DS} are shown in Figure 11. Figure 12 presents the measured output voltage V_{OUT} and output current I_{OUT} ; their measured mean values were approximately 36 V and 2 A, respectively. Figure 13 shows measured ripple waveforms of output voltage $V_{OUT-ripple}$ and output current $I_{OUT-ripple}$.

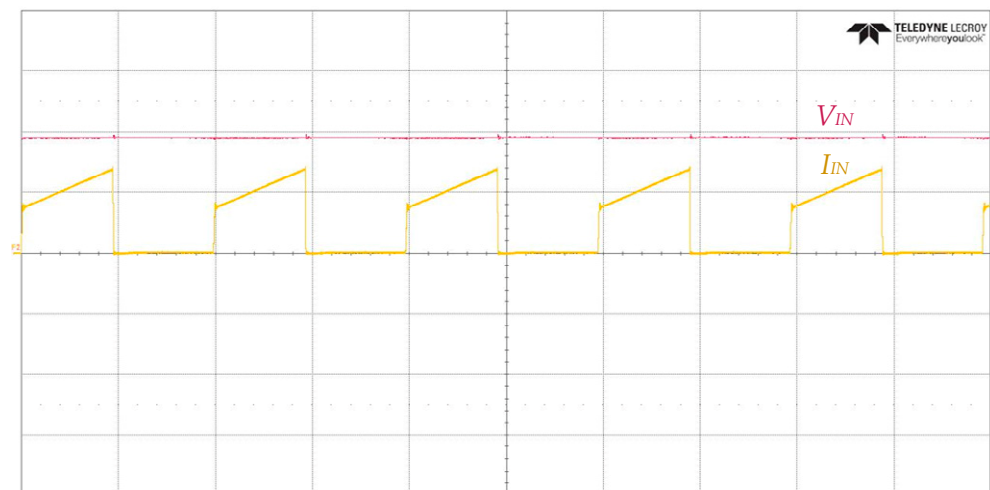


Figure 10. Measured input voltage V_{IN} (25 V/div) and input current I_{IN} (2 A/div); time scale: 10 μ s/div.

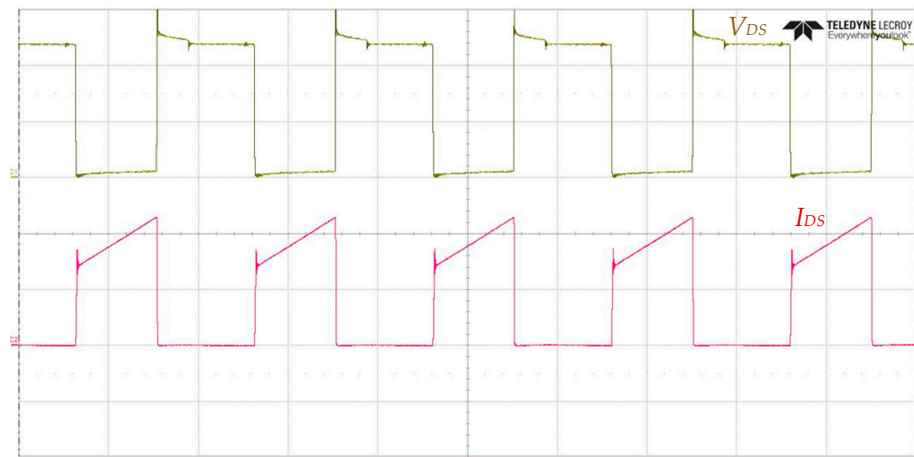


Figure 11. Measured switch voltage V_{DS} (20 V/div) and current I_{DS} (2 A/div); time scale: 10 μ s/div.

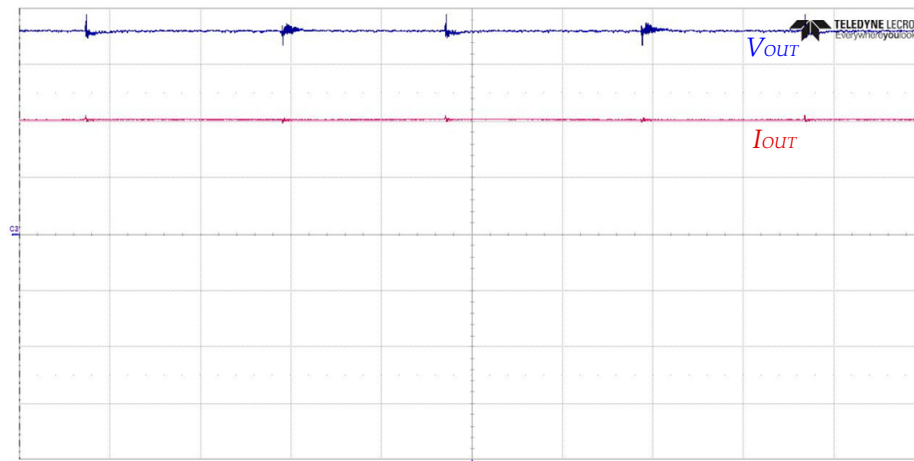


Figure 12. Measured output voltage V_{OUT} (10 V/div) and output current I_{OUT} (1 A/div); time scale: 5 μ s/div.

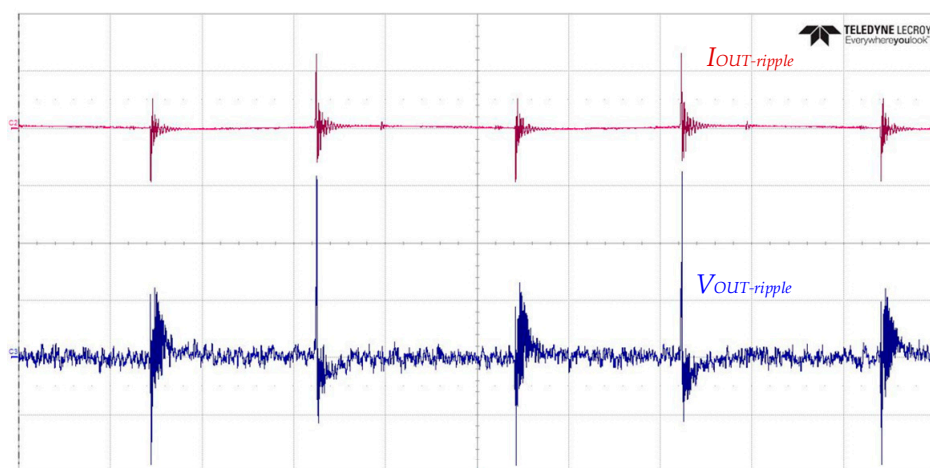


Figure 13. Measured ripple waveforms of output voltage $V_{OUT-ripple}$ (1 V/div) and output current $I_{OUT-ripple}$ (50 mA/div); time scale: 5 μ s/div.

Table 3 shows the measured output voltage ripple and output current ripple of the proposed LED streetlight driver circuit applied to a DC-input voltage of 48 V. The mean value and peak-to-peak value of the output voltage were 36.014 V and 5.137 V, respectively. In addition, the mean value and peak-to-peak value of the output current were 2.024 A

and 112.24 mA, respectively. Moreover, the ripple factor of the output voltage (current) was obtained by dividing the peak-to-peak value by the mean value of the output voltage (current). According to this table, the measured output voltage ripples and current ripples were 14.266% and 5.545%, respectively. Figure 14 presents a photograph of the proposed driver circuit supplying the experimental LED streetlight module with a DC-input voltage source of 48 V.

Table 3. Measured output voltage ripple and output current ripple in the proposed LED streetlight driver circuit.

Parameters	Values
Mean value of the output voltage	36.014 V
Peak-to-peak value of the output voltage	5.137 V
Ripple factor of the output voltage	14.266%
Mean value of the output current	2.024 A
Peak-to-peak value of the output current	112.24 mA
Ripple factor of the output current	5.545%

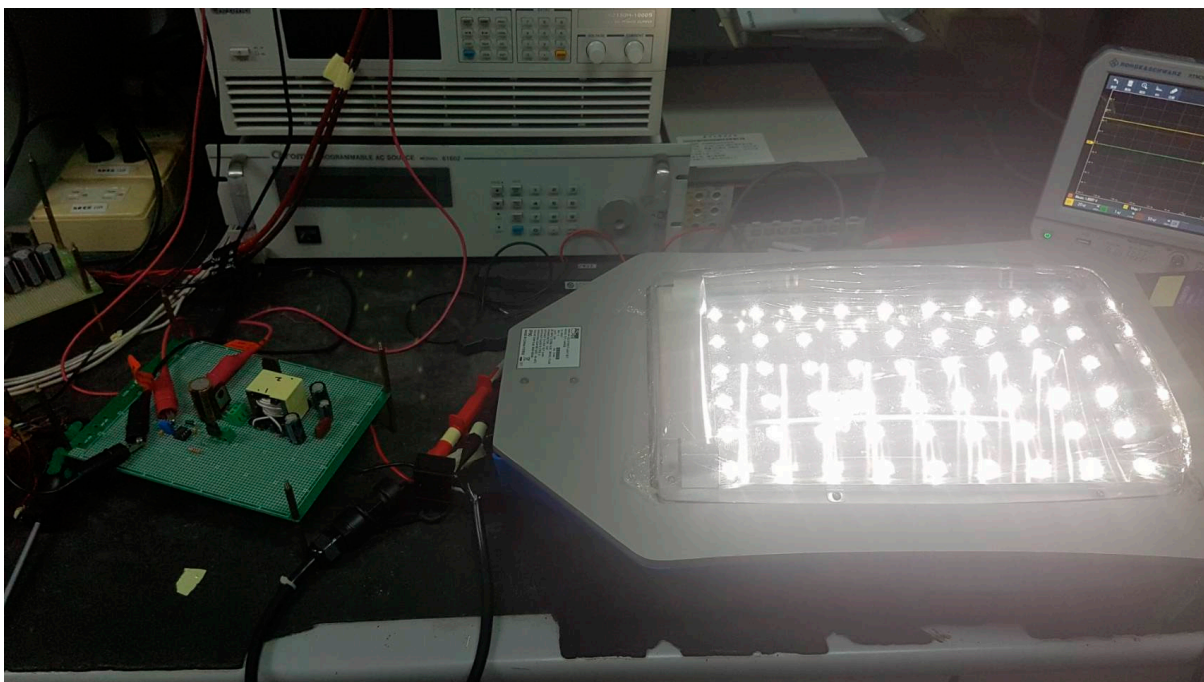


Figure 14. Photograph of supplying the experimental LED streetlight module using the proposed driver circuit with a DC-input voltage source of 48 V.

Table 4 shows a comparison between the DC–DC LED driver in [26], which supplied an 8 W-rated power with an input DC voltage of 12 V, and the proposed driver, which supplied a 72 W-rated power with an input DC voltage of 48 V. As can be seen from Table 4, both LED drivers used a single power switch, two capacitors, and a magnetic element; only two diodes were required in the proposed driver compared to the three diodes required in [26]. In addition, the circuit efficiency of the proposed LED driver was slightly better than that of the driver in [26].

Table 4. Comparisons between the existing DC–DC LED driver in [26] and the proposed driver.

Item	Existing DC–DC LED Driver in Reference [26]	Proposed DC–DC LED Driver
Circuit Topology	Buck converter with coupled inductors	Integration of a buck converter and a flyback converter
Input DC Voltage	12 V	48 V
Output Power	8 W (8 V/1 A)	72 W (36 V/2 A)
Number of Required Switches	1	1
Number of Required Capacitors	2	2
Number of Required Magnetic Elements	1	1
Number of Required Diodes	3	2
Measured Circuit Efficiency	91%	91.8%

5. Conclusions

This study proposed and implemented an LED streetlight driver applied for a DC input voltage source, integrating a buck converter with a flyback converter into a single-stage power conversion topology with the function of recovering the leakage inductance energy from the converter. In addition, the proposed circuit architecture reduced the number of power switches and components used, reduced the cost of the driver circuit, and improved the energy conversion efficiency. A prototype driver was developed and tested to supply a 72 W LED streetlight module with a rated output voltage of 36 V and a rated output current of 2 A with a DC-input voltage of 48 V. The experimental results for the presented LED streetlight driver circuit demonstrated high circuit efficiency (>91%), and the ripple factors of output voltage and output current were smaller than 15% and 6%, respectively. In the future, by redesigning and adjusting the circuit parameters, the DC–DC LED streetlight driver proposed in this paper can be applied to LED streetlights of different wattages. In addition, the proposed driver can be applied to a DC-input voltage source, such as a solar photovoltaic panel or a battery, and is suitable for LED street lighting applications.

Author Contributions: C.-A.C. developed and designed the circuit topology; C.-H.C., H.-L.C. and E.-C.C. arranged and performed circuit simulations; Y.-R.L. and L.-F.L. carried out the prototype driver circuit, and measured as well as analyzed experimental results with guidance from C.-A.C.; C.-A.C. revised the manuscript for submission. All authors have read and agreed to the published version of the manuscript.

Funding: This research was funded by the National Science and Technology Council (NSTC) of Taiwan for its grant numbers MOST 110-2221-E-214-014 and MOST 111-2221-E-214-011.

Institutional Review Board Statement: Not applicable.

Informed Consent Statement: Not applicable.

Data Availability Statement: Not applicable.

Acknowledgments: The authors would like to express their greatest and sincerest thanks to the National Science and Technology Council (NSTC) of Taiwan for grant numbers MOST 110-2221-E-214-014 and MOST 111-2221-E-214-011.

Conflicts of Interest: The authors declare no conflict of interest.

References

- Ocana-Miguel, A.; Andres-Diaz, J.R.; Hermoso-Orzáez, M.J.; Gago-Calderón, A. Analysis of the Viability of Street Light Programming Using Commutation Cycles in the Power Line. *Sustainability* **2018**, *10*, 4043. [[CrossRef](#)]
- Long, X.; Zhou, J.; Liao, R. Development of street lighting system-based novel high-brightness LED modules. *IET Optoelectron.* **2009**, *3*, 40–46. [[CrossRef](#)]
- Allwyn, R.G.; Al Abri, R.; Malik, A.; Al-Hinai, A. Economic Analysis of Replacing HPS Lamp with LED Lamp and Cost Estimation to Set Up PV/Battery System for Street Lighting in Oman. *Energies* **2021**, *14*, 7697. [[CrossRef](#)]

4. Kerbiriou, C.; Barré, K.; Mariton, L.; Pauwels, J.; Zissis, G.; Robert, A.; Le Viol, I. Switching LPS to LED Streetlight May Dramatically Reduce Activity and Foraging of Bats. *Diversity* **2020**, *12*, 165. [[CrossRef](#)]
5. Robles, J.; Zamorano, J.; Pascual, S.; de Miguel, A.S.; Gallego, J.; Gaston, K.J. Evolution of Brightness and Color of the Night Sky in Madrid. *Remote. Sens.* **2021**, *13*, 1511. [[CrossRef](#)]
6. Arias, M.; Lamar, D.G.; Linera, F.F.; Balocco, D.; Diallo, A.A.; Sebastián, J. Design of a Soft-Switching Asymmetrical Half-Bridge Converter as Second Stage of an LED Driver for Street Lighting Application. *IEEE Trans. Power Electron.* **2012**, *27*, 1608–1621. [[CrossRef](#)]
7. Sauerlander, G.; Hente, D.; Radermacher, H.; Waffenschmidt, E.; Jacobs, J. Driver electronics for LEDs. In Proceedings of the IEEE 41th IAS Annual Meeting, Tampa, FL, USA, 8–12 October 2006; pp. 2621–2626.
8. Alharbi, F.; Almoshageh, M.I.; Ibrahim, A.H.; Haider, H.; Elmadina, A.E.M.; Alfallaj, I. Performance Appraisal of Urban Street-Lighting System: Drivers' Opinion-Based Fuzzy Synthetic Evaluation. *Appl. Sci.* **2023**, *13*, 3333. [[CrossRef](#)]
9. Muneer, A.; Fayyaz, A.; Iqbal, S.; Jabbar, M.W.; Qaisar, A.; Farooq, F. Single Stage Active Power Factor Correction Circuit for Street LED Light with Battery Backup. *J. Eng. Res.* **2021**, *12*, 69. [[CrossRef](#)]
10. Adolfo, L.-M.J.; Jesús, H.-O.M.; Paulo, B. LCA Streetlight Study for Circular Economic to Local Scale. *Proceedings* **2020**, *52*, 6. [[CrossRef](#)]
11. Lozano-Miralles, J.A.; Hermoso-Orzáez, M.J.; Gago-Calderón, A.; Brito, P. LCA Case Study to LED Outdoor Luminaries as a Circular Economy Solution to Local Scale. *Sustainability* **2020**, *12*, 190. [[CrossRef](#)]
12. Cheng, C.-A.; Cheng, H.-L.; Chang, C.-H.; Chang, E.-C.; Hung, W.-S.; Lai, C.-C.; Lan, L.-F. A Single-Stage High Power Factor Power Supply for Providing an LED Street-Light Lamp Featuring Soft-Switching and Bluetooth Wireless Dimming Capability. *Energies* **2021**, *14*, 477. [[CrossRef](#)]
13. Hermoso-Orzáez, M.J.; Lozano-Miralles, J.A.; Lopez-Garcia, R.; Brito, P. Environmental Criteria for Assessing the Competitiveness of Public Tenders with the Replacement of Large-Scale LEDs in the Outdoor Lighting of Cities as a Key Element for Sustainable Development: Case Study Applied with PROMETHEE Methodology. *Sustainability* **2019**, *11*, 5982. [[CrossRef](#)]
14. Kolla, H.R.; Vishwanathan, N.; Murthy, B.K. Independently Controllable Dual-Output Half-Bridge Series Resonant Converter for LED Driver Application. *IEEE J. Emerg. Sel. Top. Power Electron.* **2022**, *10*, 2178–2189. [[CrossRef](#)]
15. Cheng, C.A.; Chang, C.H.; Cheng, H.L.; Tseng, C.H. A novel single-stage LED driver with coupled inductors and interleaved-PFC. In Proceedings of the IEEE ICPE ECCE-Asia, Seoul, Republic of Korea, 1–5 June 2015; pp. 1240–1245.
16. Deshpande, T.; Das, S.; Chavan, H.; Hangloo, A.K.; Jadhav, S. Solar Powered LED Street Lighting with Digital Control for Dimming operation. In Proceedings of the 2021 4th Biennial International Conference on Nascent Technologies in Engineering (ICNTE), Navi Mumbai, India, 15–16 January 2021; pp. 1–5.
17. Zhang, Y.; Ma, D. A Single-Stage Solar-Powered LED Display Driver Using Power Channel Time Multiplexing Technique. *IEEE Trans. Power Electron.* **2015**, *30*, 3772–3780. [[CrossRef](#)]
18. Kathiresan, R.; Xiong, T.M.; Panda, S.K.; Das, P.; Reindl, T. A non-isolated converter design with time-multiplexing control topology for un-binned high-power LEDs in parallel operation for off-grid solar-PV streetlamps. In Proceedings of the 2016 IEEE International Conference on Sustainable Energy Technologies (ICSET), Hanoi, Vietnam, 14–16 November 2016; pp. 359–363.
19. Xu, H.; Wen, H.; Li, X. Design and evaluation of a solar based single inductor multiple outputs LED lighting. In Proceedings of the International Conference on Renewable Power Generation (RPG 2015), Beijing, China, 17–18 October 2015; pp. 1–5.
20. Ocenasek, J.; Bednar, B.; Tyrpekl, M.; Michalik, J.; Kosan, T. Design of Two-Channel LED Stand-Alone Solar Lamp Driver Prototype for Biodynamic Application. In Proceedings of the 2022 IEEE 20th International Power Electronics and Motion Control Conference (PEMC), Brasov, Romania, 25–28 September 2022; pp. 691–696.
21. Jiang, X. Innovation to brisbane city council street lighting system with solar powered LED: A techno-economic feasibility study. In Proceedings of the 2016 Australasian Universities Power Engineering Conference (AUPEC), Brisbane, QLD, Australia, 25–28 September 2016; pp. 1–6.
22. Ramprasad, S.; Raj, S.; Wei, H.J.; Wong, J.K.C.; Mueller, T.; Aberle, A.G. Implementation of a novel LED based light soaking system for solar cell characterization. In Proceedings of the 2018 IEEE 7th World Conference on Photovoltaic Energy Conversion (WCPEC) (A Joint Conference of 45th IEEE PVSC, 28th PVSEC & 34th EU PVSEC), Waikoloa, HI, USA, 10–15 June 2018; pp. 2234–2236.
23. Chen, Y.; Nan, Y.; Kong, Q. A Loss-Adaptive Self-Oscillating Buck Converter for LED Driving. *IEEE Trans. Power Electron.* **2012**, *27*, 4321–4328. [[CrossRef](#)]
24. Corradini, L.; Spiazzi, G. A High-Frequency Digitally Controlled LED Driver for Automotive Applications with Fast Dimming Capabilities. *IEEE Trans. Power Electron.* **2014**, *29*, 6648–6659. [[CrossRef](#)]
25. Pollock, A.; Pollock, H.; Pollock, C. High Efficiency LED Power Supply. *IEEE J. Emerg. Sel. Top. Power Electron.* **2015**, *3*, 617–623. [[CrossRef](#)]
26. Pouladi, F.; Farzanehfard, H.; Adib, E.; Le Sage, H. Single-Switch Soft-Switching LED Driver Suitable for Battery-Operated Systems. *IEEE Trans. Ind. Electron.* **2019**, *66*, 2726–2734. [[CrossRef](#)]
27. Tseng, S.-Y.; Fan, J.-H. Zeta/Flyback Hybrid Converter for Solar Power Applications. *Sustainability* **2022**, *14*, 2924. [[CrossRef](#)]
28. Kasireddy, I.; Ch, K.R. An Efficient Selective Harmonic Based Full Bridge DC-DC Converter for LED Lighting Applications. In Proceedings of the 2019 National Power Electronics Conference (NPEC), Tiruchirappalli, India, 13–15 December 2019; pp. 1–6.

29. Song, C.; Kweon, H.; Lee, U.; Kim, J.; Yang, S.; Park, J. Modeling of conducted EMI noise in an Automotive LED Driver Module with DC/DC Converters. In Proceedings of the 2019 International Symposium on Electromagnetic Compatibility—EMC EUROPE, Barcelona, Spain, 2–6 September 2019; pp. 1009–1013.
30. Wang, Y.; Alonso, J.M.; Ruan, X. A Review of LED Drivers and Related Technologies. *IEEE Trans. Ind. Electron.* **2017**, *64*, 5754–5765. [[CrossRef](#)]

Disclaimer/Publisher’s Note: The statements, opinions and data contained in all publications are solely those of the individual author(s) and contributor(s) and not of MDPI and/or the editor(s). MDPI and/or the editor(s) disclaim responsibility for any injury to people or property resulting from any ideas, methods, instructions or products referred to in the content.